REMUNOM
ISSN 2178-6925

Received: 13.01.2026 - **Accepted:** 05/06/2026
Vol: 01.03
DOI: 10.61164/7da3gw86
Pages: 1-23

ANALYSIS OF THE BENDING PROCESS OF HSLA S700MC AND AHSS S900MC STEELS

Valtenês de Souza Bossle
Federal University of Rio Grande do Sul, Brazil
E-mail: valtenes.bossle@gmail.com

Lirio Schaeffer
Federal University of Rio Grande do Sul, Brazil
E-mail: schaefer@ufrgs.br

Matheus Henrique Riffel
Federal University of Rio Grande do Sul, Brazil
E-mail: matheus.riffel@ufrgs.br

Rafael Pandolfo da Rocha
Federal University of Rio Grande do Sul, Brazil
E-mail: rafael.pandolfo@ufrgs.br

Juliano Cantarelli Toniolo
Federal Institute of Education, Science and Technology of Rio Grande do Sul, Brazil
E-mail: juliano.toniolo@caxias.ifrs.edu.br

Abstract

HSLA S700MC and AHSS S900MC steels have been increasingly used to substitute conventional steels, and further understanding of mechanical behaviors is needed. This study aims to evaluate mathematical equations for calculating the True Strain in the outer fibers of the bending zone, Springback and Bending Force that occur in the Air Bending process for these two steels, using the analytic methods of calculation and computer simulation, comparing them to the results obtained by means of experimental analysis. Four punches were used, varying the distance between the die supports and the displacement of the punch for each one of them. Experimental analysis revealed different True Strain values in the outer fibers of the bending zone. However, despite the materials having distinct mechanical properties, the values obtained through analytical calculation methods were found to be the same for both steels. While the predictability of the Springback Factor through the analytical method varied from 0.5% to 6.5% and for Bending Force the variation was from 10.0% to 38.3%.

Keywords: S700MC steel; S900MC steel; true strain, springback; computer simulation.

REMUNOM
ISSN 2178-6925

Received: 13.01.2026 - **Accepted:** 05/06/2026
Vol: 01.03
DOI: 10.61164/7da3gw86
Pages: 1-23

1. Introduction

High Strength Low Alloy (HSLA) steel S700MC, as well as Advanced High Strength Steel (AHSS) S900MC, enable reduction thickness and consequent weight reduction, without affecting the safety and strength of the part, due to greater resistance (SSAB, 2023).

These are hot-rolled structural steels with minimum Engineering Yield Stress (σ_e) of 700 MPa and 900 MPa respectively and they allow manufacturing lighter, stronger parts (USIMINAS, 2023).

They are applied to a large variety of components, such as for example, tower crane parts, road and agricultural implements, extra lightweight chassis and longitudinal girders, stakes, crane booms, as well as structural components, parts used to load cargo, in general (ULSAB, 2023).

One of the challenges for the mechanical forming process of metal sheets from high strength steels is to achieve the predictability of the True Strain in the outer bending zone, the Springback Factor and the Bending Force (Farsi; Arezoo, 2011).

One of the great problems of the mechanical forming process for high strength steel sheets was to eliminate cracks and cracking, due to their low deformability. It is necessary to achieve control of stability and dimensional precision, and Springback is one of the parameters that render this control difficult. Variations of the stresses present in the Bending cause Springback, since tensile stresses occur on the outer surface, on the other hand, on the inner surface of the bend stress is due to compression (Dieter, 1981).

The higher value of both stresses occurs on the surface of the material and diminishes as it approaches the center of the Sheet thickness (s), becoming zero as it reaches the neutral axis. In this region the material creates a narrow elastic range on both sides of the neutral axis and, as it moves towards the surface, stresses above the engineering yield stress limit are obtained, causing plastic and permanent strain. When the Punch moves away the elastic range tends to return to its original flat condition, but this is not possible, due to the restrictions caused by

REMUNOM
ISSN 2178-6925

Received: 13.01.2026 - **Accepted:** 05/06/2026
Vol: 01.03
DOI: 10.61164/7da3gw86
Pages: 1-23

the plastic strain zones (Perka, 2022).

The geometrical distortion which makes it difficult or even impossible to assemble the parts is often caused by Springback and is a challenge to the project (Vorkov, 2018).

A few parameters of the air bending process such as Sheet thickness (*s*), Punch Radius (r_p), Bending Force (F_d), Distances between Supports (w) and Maximum Displacement of the Punch (*h*), as well as some properties of the material such as Anisotropy Index (*r*), Hardening Coefficient (*n*), microstructural aspect and lubrication conditions, among others, influenced Springback. Analytic expressions in general do not take all these parameters into account (Narayanasamy; Padmanabhan, 2012).

Figure 1 shows schematics with air bending and the main parameters involved in this type of bending (Livatyali; Altan, 2001).

Figure 1: Shows air bending process and the main parameters of this process.

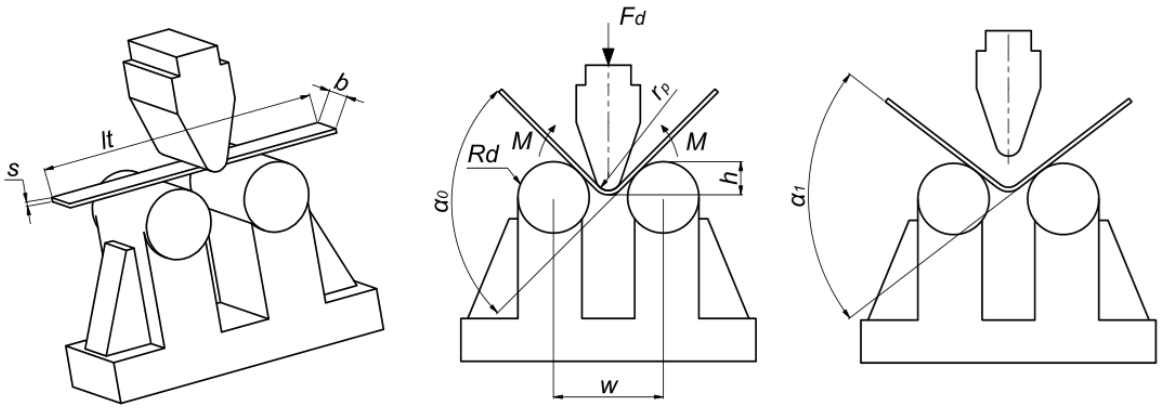

Source: Elaborated by authors (2026).

The Maximum Bending Force ($F_{máx.}$) occurs at the end of the process, corresponding to the Angle of Bending before Springback (α_0). When the tool is removed, releasing the contact surface, force is released and, consequently, the spring effect occurs, reflected in the change of the Angle of Bending after Springback (α_1) (Aerens; Masselis, 2000; Yang et al., 2011).

This study aims to evaluate the use analytic expressions in the manufacturing

REMUNOM
ISSN 2178-6925

Received: 13.01.2026 - **Accepted:** 05/06/2026
Vol: 01.03
DOI: 10.61164/7da3gw86
Pages: 1-23

project of the air bending manufacturing process. Currently, due to its low cost and quickly obtained results in supporting the performance and optimization of manufacturing projects this formulism is still often used.

This study aims to evaluate the use of analytic expressions for determining the True Strain (φ_x) in the outer bending zone and in the length direction (x) of the sheet, the Springback Factor (K) and the Bending Force (F_d) that occur in the air bending process for these two steels. Currently, due to its low cost and the quickly obtained results in supporting the performance and optimization of manufacturing projects, the analytical method is still frequently used. (Arola et al., 2015).

2. Methodology

2.1 Determination of the mechanical properties

In order to determine the mechanical properties a tensile test was performed utilizing 3.0 mm thick sheets (s) of S700MC and S900MC steels. This test was done to construct the Engineering Curves and Flow Stress Curves. The dimensions and geometry used for the test specimens were of the rectangular type, and are in accordance with the requirement of ABNT NBR 6892-1-2013 standards, as well as of the procedures to carry out this test. The equipment utilized to perform the tensile test was a 100 kN universal test equipment of the EMIC brand.

Figure 2 shows the graph of the Engineering Curves for the S700MC and S900MC steels. Looking at the results of the tensile tests, it was found that Engineering Yield Stress (σ_e) were 861.5 MPa for S700MC steel and 1048.4 MPa for S900MC steel. On the other hand, Maximum stress (R_m), was 919.8 MPa for S700MC steel and 1117.4 MPa for S900M steel, with respective Relative Strains (ε) of 6.3% and 2.0%. The low deformability of S900MC steel should be emphasized, as shown in Figure 2.

The Flow Stress Curves of the two steels were determined by utilizing the data of strength and instantaneous areas obtained during the tensile tests considering only the uniform plastic strain Zone. Figure 3 shows the flow stress curves for S700MC and S900MC steels.

REMUNOM
ISSN 2178-6925

Received: 13.01.2026 - **Accepted:** 05/06/2026
Vol: 01.03
DOI: 10.61164/7da3gw86
Pages: 1-23

Figure 2: Engineering stress-strain curves σ x ε.

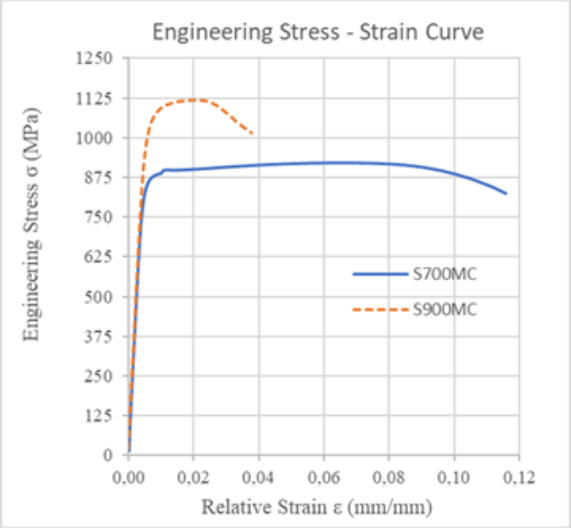

Source: Elaborated by authors (2026).

Figure 3: Flow stress curves *kf* x *φ*.

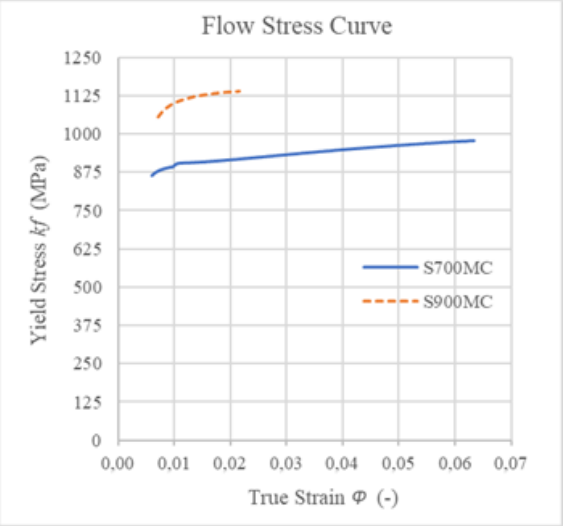

Source: Elaborated by authors (2026).

The flow stress equations of S700MC and S900MC steels were determined according to the proposal of Ludwik - Hollomon, utilizing the data of Maximum Stress (R_m) and of the respective Relative Strain (ε) corresponding to this point. After this the True Stresses *(kf)* and True Strains (φ) were calculated using Equations 1 and 2 (Lange, 1985).

$$kf = \sigma(1 + \varepsilon) \quad \text{Eq. 1}$$

$$\varphi = \ln(1 + \varepsilon) \quad \text{Eq. 2}$$

Equation 3 of Ludwik-Hollomon was used, into which the values of the Hardening Index *(n)*, True Strain (φ) and True Stress (kf), were inserted, corresponding to the point of Maximum Stress (R_m) and the respective Relative Strain (ε), and then the values of the Material Resistance Constant (*C*) of these two materials were determined. Thus, Equation 4 and 5 were determined, which describe the Flow Stress Curves of these two steels.

Ludwik-Hollomon equation $kf = C.\varphi^n$ Eq. 3

REMUNOM
ISSN 2178-6925

Received: 13.01.2026 - **Accepted:** 05/06/2026
Vol: 01.03
DOI: 10.61164/7da3gw86
Pages: 1-23

S700MC	$kf = 1160{,}2.\varphi^{0{,}061}$	Eq. 4
S900MC	$kf = 1233{,}3.\varphi^{0{,}020}$	Eq. 5

2.2 Methods of analysis

2.2.1 Experimental analysis

To perform the Bending experiment, 36 tests specimens were manufactured from S700MC steel and 36 from S900MC steel, utilizing Sheet thickness (*s*) of 3mm.

As advised by the EN 10149-3 standard for an S700MC steel sheet, the Minimum radius of bending (r_{min}) is 1.5s (4.5mm). On the other hand, for an S900MC steel sheet, with a 3mm thickness (*s*), the Minimum radius of bending (r_{min}) is 3.5s (10.5mm), and this guidance is for angles before Springback (α_0) ≤ 90°, for these two steels (EN 10149-2, 2013).

For the two steels the same Punch Radii (r_p) were used, 3, 6, 9 and 12mm and, for each Punch, 9 test specimens were used to compare the True Strain (φ_x) values in the outer region of Bending and the Springback Factor (*K*) between the two steels studied. Table 1 shows the fixed parameters utilized in the air bending experiment.

Table 1: Fixed parameters utilized in the air bending experiment.

Bending angle before Springback, α_0 (°)	90
Punch velocity, *V* (mm/min)	10
Sheet thickness, *s* (mm)	3
Width of the test specimen, *b* (mm)	30
Length of the test specimen, *L* (mm)	210
Die radius, R_d (mm)	25

Source: Elaborated by authors (2026).

The Distance between the supports (*w*) was determined using Equation 6, which is adapted from the ABNT NBR 7438:2022 Standard.

$$w = (2 * r_p) + (3 * s) + (2 * R_d) \quad \text{Eq. 6}$$

The values of Maximum Displacement of the Punch (*h*) were obtained through a geometrical representation, utilizing the INVENTOR software, where the 4

REMUNOM
ISSN 2178-6925

Received: 13.01.2026 - **Accepted:** 05/06/2026
Vol: 01.03
DOI: 10.61164/7da3gw86
Pages: 1-23

Radiuses of the Punch (r_p) and the 90° Bending Angle before Springback (α_0) were represented.

For each Punch Radius (r_p), the Distance between the Supports (*w*) and the Maximum Displacement of the Punch *(h)* varied, and for all representations the Die radius (R_d) and the thickness of the sheet (*s*) were equal. Figure 1 is the schematic representation of the Air Bending experiment.

Table 2 shows the values of Distance between the Support *(w)* and Maximum Displacement of the Punch *(h)* for each Punch Radius (r_p).

Table 2: Values of Maximum Displacement of the Punch (*h*) and the Distance Between the Supports (w) for each Punch Radius (r_p).

Material	Punch Radius r_p (mm)	Distance Between the Supports *w* (mm)	Maximum Displacement of the Punch *h* (mm)
S700MC and S900MC	3	65	20
	6	71	21
	9	77	23
	12	83	25

Source: Elaborated by authors (2026).

The True Strain (φ_x) in the outer region of the bending was determined using the mesh visioplasticity method, which is widely employed in plastic forming studies. Before performing the bending tests, regular circular grids with an Initial diameter (d_0) of 2.5 mm were engraved on the surface of the test specimens, located in the region that was subsequently subjected to maximum deformation.

After performing the bending tests, these circles deformed became ellipses, whose elongation along the major axis was measured using a flexible measuring grid. The True Strain (φ_x) was then calculated from the ratio between the initial and final lengths of the major axis of the ellipse, assuming a plane strain condition in the analyzed zone, according to a methodology consolidated in the technical literature.

For experimental analysis of the bending tests, a universal testing machine of 600 kN from EMIC was used to perform the air bending experiment, as shown in Figure 4. The test specimens were bending, placing the face with the engraved circles against the die supports and opposite the punch.

REMUNOM
ISSN 2178-6925

Received: 13.01.2026 - **Accepted:** 05/06/2026
Vol: 01.03
DOI: 10.61164/7da3gw86
Pages: 1-23

Figure 4: Air bending experiment of one of the test specimens.

Source: Elaborated by authors (2026).

After the complete removal of the punch load, the Springback angle (α_1) was obtained experimentally by geometrically measuring the final angle of each specimen, using a precision angle measuring instrument.

With these measured values, the average Springback Factor (*K*) was calculated for each Punch Radius (r_p) used in the bending experiment, using Equation 7, proposed by Dieter (1981), defined as the ratio between the Angle after springback (α_1) and the Angle before springback (α_0), a methodology widely adopted in free air bending experiments (Schaeffer; Nunes; Brito, 2017; Rodrigues; Martins, 2010). The angle before springback (α_0) was defined as 90°, as shown in Table 1.

$$K = \frac{\alpha_1}{\alpha_0} \qquad \text{Eq. 7}$$

The Maximum Bending Force ($F_{máx.}$) was extracted directly from the data acquisition system of the universal testing machine used in the experiments.

During the experiment, force values were continuously recorded as a function of displacement of the punch. The Maximum Bending Force ($F_{máx.}$) was identified as the highest value recorded immediately before the start of unloading, corresponding to the end of the punch stroke and the imposed bending angle.

This value was considered representative of the Maximum Bending Force ($F_{máx.}$) for each experimental condition analyzed.

REMUNOM
ISSN 2178-6925

Received: 13.01.2026 - **Accepted:** 05/06/2026
Vol: 01.03
DOI: 10.61164/7da3gw86
Pages: 1-23

2.2.2 Analytic methods for calculation

The same parameters of the experimental analysis were utilized in order to perform the analytic calculations using mathematical equations.

The True Strains (φ_x) in the outer bending zone and in the length direction (*x*) of the sheet as shown in Figure 5, were calculated using Equations 8 proposed by Lange (1985) and 9 proposed by Hosford and Caddel (2010), that correlates the Sheet thickness (*s*), Punch Radius (r_p), Bending radius of the midline (r_m), the Position of the fibers in the sheet (*y*) as being s/2, the Bending arc length (l_s) and the Length of the fiber (l) located in position *y* (Hosford and Caddell, 2011).

Figure 5: Representation of the Bending region and variables involved in calculating the True Strain (φ_x).

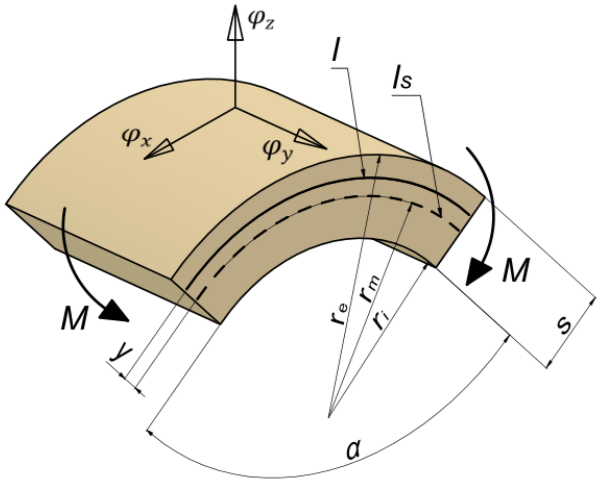

Source: Adapted from Hosford and Caddell (2011).

The True Strains (φ_y) in the direction of the Sheet width (*b*) and (φ_z) in the direction of Sheet thickness (*s*), were not taken into account in this study. Plane Strain was considered, where $\varphi_y = \varphi_x$ and φ_z= 0 (Vorkov, et al., 2017).

$$\varphi_x = ln \sqrt{1 + \frac{s}{r_P}} \qquad \text{Eq. 8}$$

REMUNOM
ISSN 2178-6925

Received: 13.01.2026 - **Accepted:** 05/06/2026
Vol: 01.03
DOI: 10.61164/7da3gw86
Pages: 1-23

$$\varphi_x = ln\left(1 + \frac{s}{2r_m}\right) \quad \text{Eq. 9}$$

On the other hand, Equation 10 was used to calculate the Bending radius of the midline (r_m), necessary to determine the True Strain (φ_x) using Equation 9 (Rocha, et al., 2022).

$$r_m = r_p + \frac{s}{2} \quad \text{Eq. 10}$$

In order to determine the values of the analytic Springback Factor (*K*), Equation 11 proposed by Dieter (1981) can be used. Where *s* is Thickness, *b* Width, *E* the elasticity Module of the material, r_p the Punch Radius and *M* is the Bending Moment which depends on the Bending Force (F_d) and on the Distance between the supports (*w*).

$$K = 1 - \frac{12M\left(r_p + 0{,}5.s\right)}{E.b.s^3} \quad \text{Eq. 11}$$

Equation 6 was used to determine the Distance between the Supports (*w*), which is adapted from the ABNT NBR 7438:2022 Standard. Now, to calculated the Bending Moment (*M*) was used Equation 12 proposed by Martins and Rodrigues (2010).

$$M = \frac{F_d.w}{4} \quad \text{Eq. 12}$$

For the Bending Force (F_d), among those found in the literature, was used Equation 13 proposed by SSAB (2021).

$$F_d = \frac{R_m.b.s^2}{(w - R_d - r_p)} \quad \text{Eq. 13}$$

REMUNOM
ISSN 2178-6925

Received: 13.01.2026 - **Accepted:** 05/06/2026
Vol: 01.03
DOI: 10.61164/7da3gw86
Pages: 1-23

2.2.3 Computer simulation

The air bending process was simulated using Simufact Forming 15® software (MSC Software Company, Hexagon), employing the finite element method to determine the stress and strain fields along the forming process.

An elastoplastic formulation suitable for high rotations and moderate strains was adopted, with a solid-shell discretization, allowing the integration of mechanical variables at multiple points along the thickness of the sheet (*s*).

The Punches and Die were considered rigid, non-deformable objects, while the sheets were considered elastoplastic objects. The contact between the tool and the workpiece was modeled using Coulomb's law of friction, with a constant Coefficient of friction μ = 0.1. The Punch velocity (*V*) was set at 19.5 mm/s, according to typical conditions of industrial bending processes (Fu; Mo; Chen, 2010).

Figure 6 illustrates the initial (a) and final (b) positions of the punch, according to procedures consolidated in the literature on numerical simulation of forming processes (Fu; Mo; Chen, 2010) (Altan; Tekkaya, 2012; Hosford; Caddell, 2011).

Figure 6: Representation of the initial (a) and final (b) positions of the Punch.

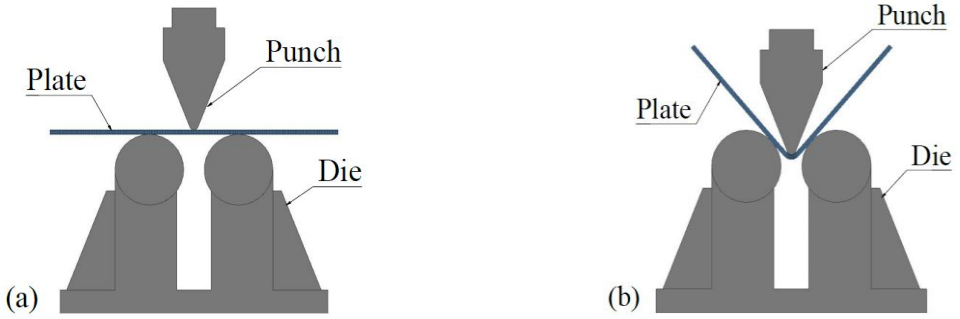

Source: Elaborated by authors (2026).

The plastic behavior of the material was described by the Ludwik–Hollomon constitutive model, in which the yield stress evolves as a function of the equivalent plastic strain according to a power law, fitted from experimental data. This approach allows for the accurate representation of material work hardening and its influence on bending strength, as well as on the stress distribution along the Sheet thickness (*s*). The springback was evaluated during the unloading phase of the simulation,

REMUNOM
ISSN 2178-6925

Received: 13.01.2026 - **Accepted:** 05/06/2026
Vol: 01.03
DOI: 10.61164/7da3gw86
Pages: 1-23

being determined by the elastic properties and the history of plastic strains imposed during the computer simulation. Based on the results obtained using the tensile tests, the mechanical properties of S700MC and S900MC steels were entered into the software, as shown in Table 3.

Table 3: Mechanical properties entered into the SIMUFACT software.

Parameters	Material	
Blank material	S700MC	S900MC
Engineering Yield Stress, σ_e (MPa)	861.5	1048.4
Maximum Stress, R_m (MPa)	919.8	1117.4
Anisotropy Index, *r* (-)	1.61	1.78
Density, *ρ* (g/cm³)	7.85	7.85
Elasticity Modulus, *E* (GPa)	201.5	200.7
Poisson coefficient, *v* (-)	0.285	0.270
Material Resistance Constant, *C* (MPa)	1160,2	1233.3
Hardening Index, *n* (-)	0.061	0.020
Coefficient of friction, (*μ*)	0.1	

Source: Elaborated by authors (2026).

To validate the numerical simulation, 4 of S700MC steel and 4 of the S900MC steel bending simulations were performed, one for each Punch Radius (r_p) utilized in the bending experiment, with the aiming to estimate the True Strain (φ_x) in the outer bending region and the Springback Factor (*K*) (Ledentsoy, *et al*., 2010).

To mesh convergence, a 1mm general mesh size was adopted, hexahedral type elements, Sheetmesh mesh generator, quantity of elements 18900 and the number of elements along the thickness was 3 (Ledentsoy, et al., 2010).

For the simulations, the same Punch radii (r_p) were considered, the same Distance between the supports (*w*) and the same Maximum Displacement of the Punch (*h*) utilized in the bending experiment.

3. Results and discussion

3.1 Experimental analysis

No cracks were found to have occurred for S700MC steel, in the outer region of the bend in the group of test specimens with a Punch Radius (r_p) 3mm, below the minimum specified by the EM 10149-2 standard (minimum Punch Radius (r_p) 4.5 mm).

REMUNOM
ISSN 2178-6925

Received: 13.01.2026 - **Accepted:** 05/06/2026
Vol: 01.03
DOI: 10.61164/7da3gw86
Pages: 1-23

Based on the experimental results presented in the article, it is observed that the S900MC steel exhibited behavior sensitive to the imposed bending radius, in accordance with the normative recommendations.

In the outer region of the bend, the test specimens subjected to a Punch Radius (r_p) lower than the minimum specified by the EN 10149-2 standard, 3.5 times the thickness, that corresponding to 10.5 mm for Sheet thickness (s) of 3 mm, showed the occurrence of cracks when a Punch Radius (r_p) of 3 mm was used, as illustrated in Figure 7. This behavior is associated with the high True Strains concentrated in the outer fibers of the bend, typical of AHSS steels with lower ductility. On the other hand, no cracks were observed in the specimens bent with Punch Radius (r_p) of 6, 9, and 12 mm, indicating that, for these Punch Radius (r_p), the imposed strain remains within the formability limit of the material, guaranteeing the geometric and structural integrity of the bent parts.

Figure 7: Occurrence of cracks in the outer bent region of S900MC steel for a Punch Radius (r_p) of 3mm.

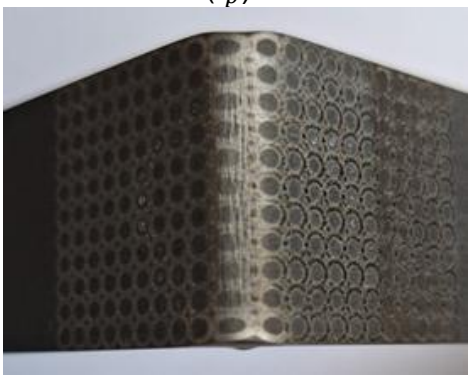

Source: Elaborated by authors (2026).

After the bending experiment, as shown in Figure 8, the True Strain (φ_x) values were measured along the length of the sheet, in the outer bending region and in the length direction (x) of the test specimens, using the flexible and transparent ruler for measuring strains.

Looking at the results of the experiment for the two steels studied in this article, it was observed that the larger the Punch Radius (r_p), the smaller is the Springback Factor (K).

REMUNOM
ISSN 2178-6925

Received: 13.01.2026 - **Accepted:** 05/06/2026
Vol: 01.03
DOI: 10.61164/7da3gw86
Pages: 1-23

Figure 8: Verification of the True Strain (φ_x) of the bended outer region.

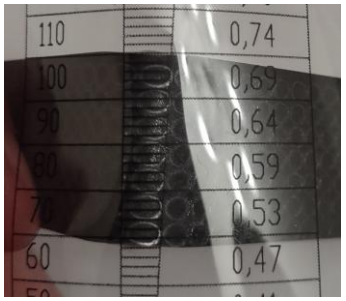

Source: Elaborated by authors (2026).

Table 4 presents the averages and standard deviations for each Punch Radius (r_p), of the experimental values of True Strain (φ_x) in the outer bending region in the length direction (*x*), Springback Factor (*K*) and Maximum Bending Force ($F_{máx.}$), for the two steels studied.

Table 4: Experimental values of the Average and Standard deviation of True Strain (φ_x), Springback Factor (K) and Maximum Bending Force ($F_{máx.}$).

Material	Punch Radius r_p (mm)	True Strain φ_x (-)		Springback Factor K (-)		Maximum Bending Force $F_{máx.}$ (N)	
		Average	Standard deviation	Average	Standard deviation	Average	Standard deviation
S700MC	3	0.36	0.009	0.909	0.005	7422	364.5
	6	0.25	0.005	0.898	0.003	5945	171.0
	9	0.18	0.004	0.897	0.003	6032	211.8
	12	0.12	0.004	0.892	0.001	7083	131.6
S900MC	3	0.44	0.018	0.912	0.001	10411	207.9
	6	0.23	0.005	0.901	0.001	11122	248.5
	9	0.17	0.005	0.880	0.001	10100	205.5
	12	0.14	0.004	0.872	0.005	9156	142.3

Source: Elaborated by authors (2026).

3.2 Analytical calculation method

For both steels, the True Strain (φ_x) in the outer bending region in the length direction (*x*), values were calculated using Equations 8 and 9. The bending radius of the centerline (r_m) was calculated using Equation 10. The values of the Springback Factor (*K*), the Bending Moment (*M*) and the Bending Force (F_d) were calculated using Equations 11, 12, and 13, and are presented in Table 5, respectively.

REMUNOM
ISSN 2178-6925

Received: 13.01.2026 - **Accepted:** 05/06/2026
Vol: 01.03
DOI: 10.61164/7da3gw86
Pages: 1-23

Table 5: Analytic values of True Strain (φ_x), Bending radius of the midline (r_m), Springback Factor (K), Bending Moment (M) and Bending Force (F_d).

Material	Punch Radius r_p (mm)	Punch adius φ_x (-)		Bending radius of the midline r_m (mm), Eq. 10	Springback Factor K (-), Eq. 11	Bending Moment M (N.mm), Eq. 12	Bending Force F_d (N), Eq. 13
		Eq. 8	Eq. 9				
S700MC	3	0,35	0.29	4.5	0.969	94142	5793
	6	0.20	0.18	7.5	0.947	95120	5359
	9	0.14	0.13	10.5	0.925	95961	4985
	12	0.11	0.11	13.5	0.903	96692	4660
S900MC	3	0.35	0.29	4.5	0.960	120461	7413
	6	0.20	0.18	7.5	0.932	121712	6857
	9	0.14	0.13	10.5	0.904	122789	6379
	12	0.11	0.11	13.5	0.876	123725	5963

Source: Elaborated by authors (2026).

3.3 Computer simulation

Figure 9 shows a computational numerical simulation of the True Strain (φ_x) of S700MC steel for a Punch Radius (r_p) of 3mm. It can be seen that the maximum True Strain (φ_x), with a value of 0.33, is located at the corners of the outer surface of the bending region (in red).

Figure 9: Computational numerical simulation of the True Strain (φ_x) of S700MC steel for a Punch Radius (r_p) of 3 mm.

Source: Elaborated by authors (2026).

REMUNOM
ISSN 2178-6925

Received: 13.01.2026 - **Accepted:** 05/06/2026
Vol: 01.03
DOI: 10.61164/7da3gw86
Pages: 1-23

Figure 10 shows the computational numerical simulation of the Angle after springback (α_1) of S700MC steel for Punch Radius (r_p) of 9 mm. The geometry of the bended sheet was generated by SIMUFACT FORMING 15® software and later transferred to the INVENTOR software, where the Angle after springback (α_1) of 83° was verified.

Figure 10: Computational numerical simulation of the Angle after springback (α_1) of S700MC steel for a Punch Radius (r_p) of 9 mm.

Source: Elaborated by authors (2026).

Table 6 shows the computer simulation values for True Strain (φ_x) in the outer bending region in the length direction (*x*), Springback Factor (*K*), and Bending Force (F_d).

Table 6: Computer simulation values for True Strain (φ_x), Springback Factor (K) and Bending Force (F_d).

Material	Punch Radius r_p (mm)	True Strain φ_x (-)	Springback Factor *K* (-)	Bending Force F_d (N)
S700MC	3	0.33	0.936	6963
	6	0.23	0.930	6505
	9	0.17	0.923	6410
	12	0.12	0.921	6370
S900MC	3	0.31	0.939	10770
	6	0.21	0.922	10548
	9	0.16	0.904	10230
	12	0.13	0.898	8538

Source: Elaborated by authors (2026).

REMUNOM
ISSN 2178-6925

Received: 13.01.2026 - **Accepted:** 05/06/2026
Vol: 01.03
DOI: 10.61164/7da3gw86
Pages: 1-23

4. Discussion

Figure 11 shows the experimental values of the True Strain (φ_x) in the outer bending region in the length direction (x) considered as a reference in this study, as well as the analytic values and those obtained by computer simulation.

Figure 11: Ratio between True Strain (φ_x) and Punch Radius (r_p) for the two steels.

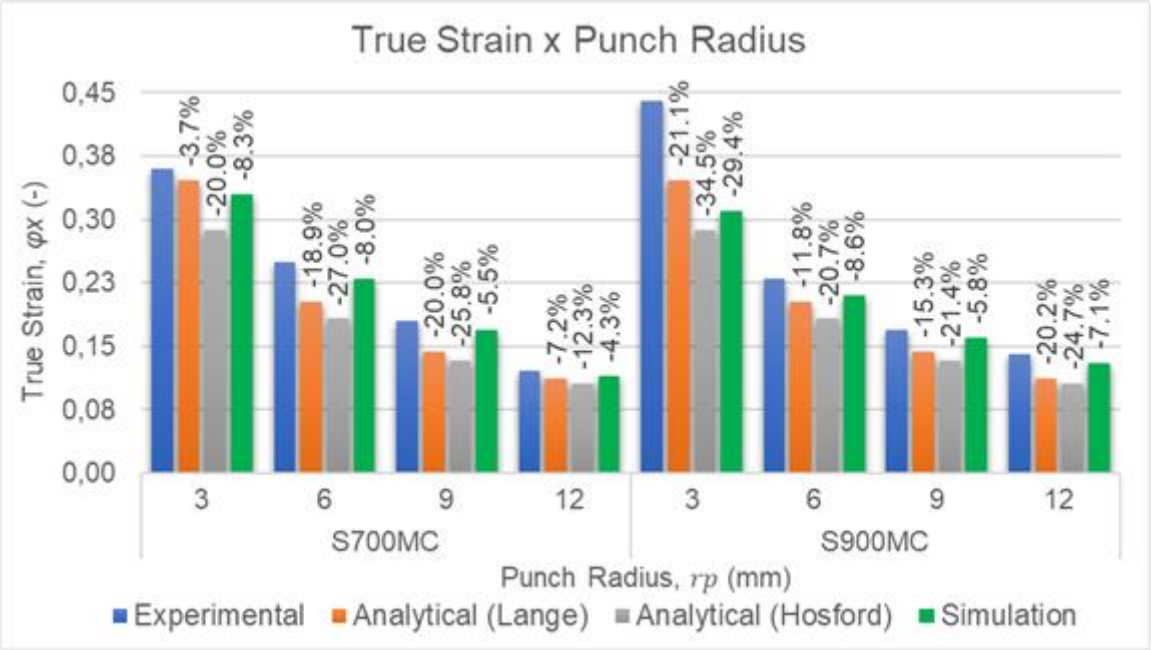

Source: Elaborated by authors (2026).

According to the experimental results presented in the graph in Figure 11, for different values of Punch Radius (r_p), Distance between Supports (w) and of Maximum of the Punch Displacement (h), different values of True Strain (φ_x) were obtained. The same occurred with the analytical methods of calculation and computational numerical simulation. However, although the two materials have different mechanical properties, it can be seen for the analytical method that the values calculated through Equation 8 and presented in Table 5 are the same for both steels, since the parameters considered in this equation are the Sheet thickness (s) and the Punch Radius (r_p). The same was also observed for the values calculated through Equation 9 and presented in Table 5, since the parameters considered in this equation are the Sheet thickness (s) and the Bending radius of

REMUNOM
ISSN 2178-6925
Received: 13.01.2026 - **Accepted:** 05/06/2026
Vol: 01.03
DOI: 10.61164/7da3gw86
Pages: 1-23

the midline (r_m). For both equations, the values diverged significantly from the experimental values.

It was observed for the test specimens that presented cracks in the S900MC steel with a Punch Radius (r_p) of 3 mm, that the True Deformation (φ_x) was high, possibly due to rupture of the material in the outer surface zone of a bend.

The graph in Figure 12 shows the values of the Springback Factor (*K*), obtained using the analytic methods of calculation and computer simulation, compared to experimental analysis, it is found that the error percentages remained below 10%.

Figure 12: Ratio between Springback Factor (*K*) and Punch Radius (r_p) for the two steels.

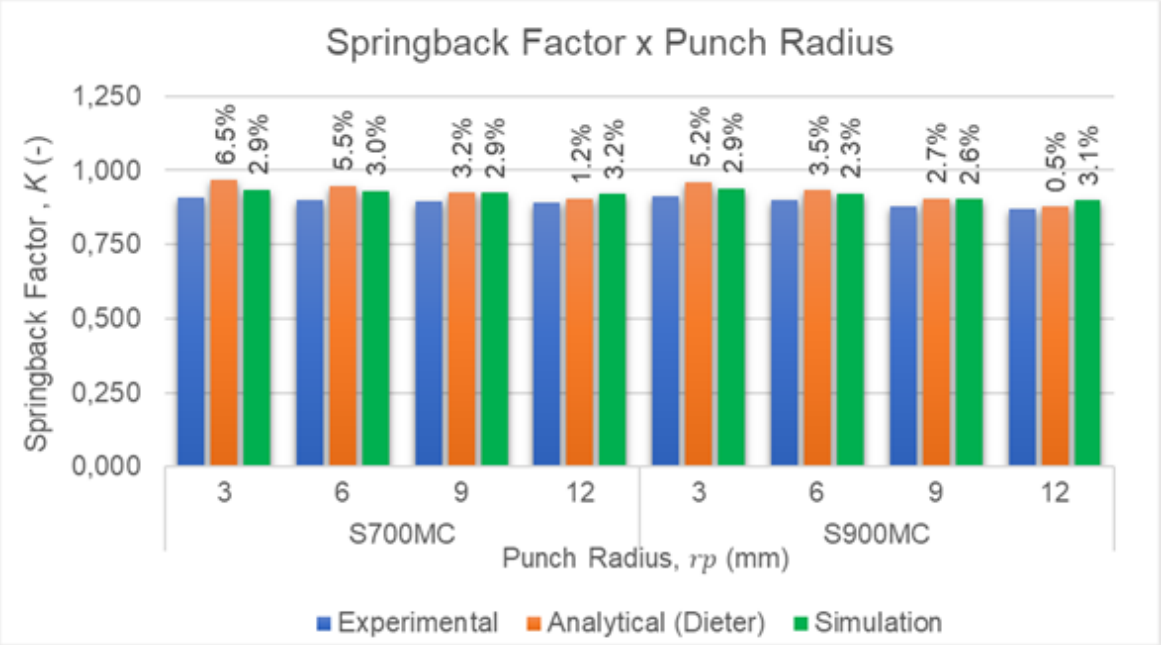

Source: Elaborated by authors (2026).

For experimental analysis, as well as for the analytic methods of calculation and computer simulation, the Springback Factor (*K*) values were seen to vary based on the variation of the parameters of the bending experiment. It is found that both for the S700MC steel and for the S900MC steel, there is a tendency to diminish the Springback Factor (*K*), as the Punch Radius (r_p) increases.

According to the results presented for Bending Force (F_d), as observed in the graph of Figure 13 for both steels, the percentage differences were between -10% to -38.3% for the values calculated using the analytical method through Equation 13

REMUNOM
ISSN 2178-6925

Received: 13.01.2026 - **Accepted:** 05/06/2026
Vol: 01.03
DOI: 10.61164/7da3gw86
Pages: 1-23

and -5.9% to 10% for computational numerical simulation compared to experimental analysis.

Figure 13: Ratio between Bending Force (F_d) and Punch Radius (r_p) for the two steels.

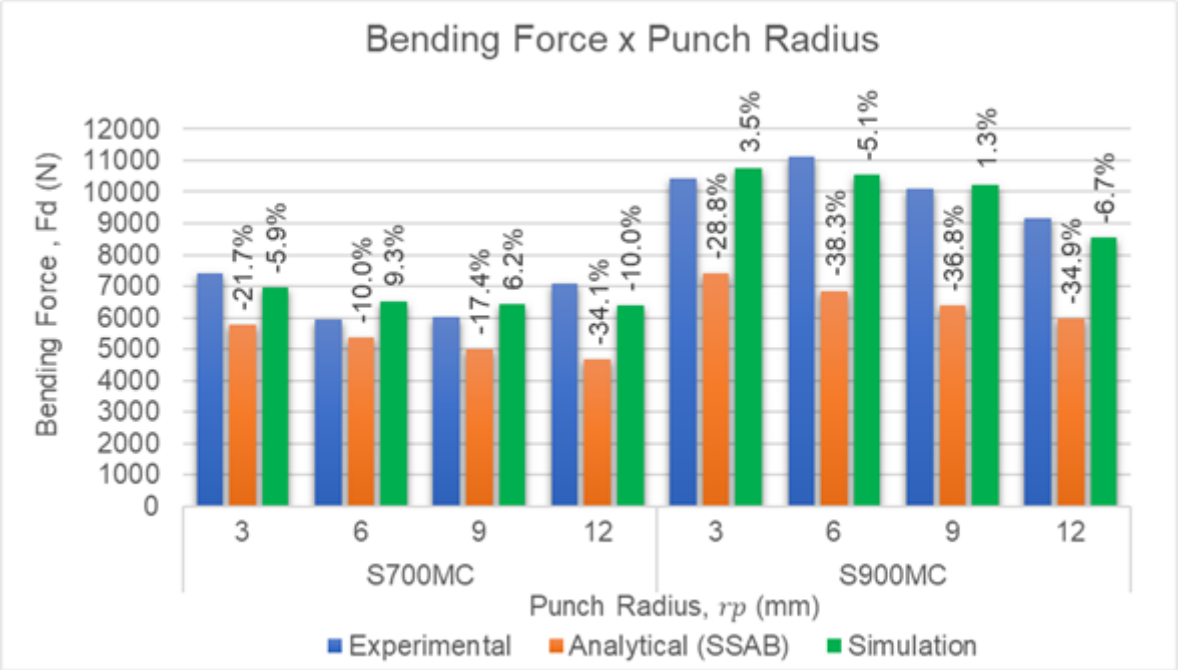

Source: Elaborated by authors (2026).

5. List of Symbols

Table 7: List of Symbols Used.

b – Width of the test specimen ..... [mm]	M – Bending Moment ..... [N.mm]
C – Material Resistance Constant ..... [MPa]	n – Hardening Index .....[-]
d_0 – Initial diameter ..... [mm]	r – Anisotropy Index .....[-]
E – Elasticity Modulus ..... [GPa]	R_d – Die radius ..... [mm]
F_d – Bending Force .....[N]	R_m – Maximum Stress ..... [MPa]
$F_{máx.}$ – Maximum Bending Force ..... [N]	r_m – Bending radius of the midline .....[mm]
h – Maximum Displacement Punch ..... [mm]	r_{min} – Minimum radius of bending ..... [mm]
K – Springback Factor .....[-]	r_p – Punch Radius ..... [mm]
k_f – True Stress ..... [MPa]	s – Sheet thickness .....[mm]
L – Length of the test specimen .....[mm]	V – Punch velocity ..... [mm/min]
l – Length of the fiber .....[mm]	w – Distance between the supports ..... [mm]
l_s – Bending arc length ..... [mm]	y – Position of the fibers in the sheet ..... [mm]

Source: Elaborated by authors (2026).

REMUNOM
ISSN 2178-6925

Received: 13.01.2026 - **Accepted:** 05/06/2026
Vol: 01.03
DOI: 10.61164/7da3gw86
Pages: 1-23

Table 8: List of Greek symbols used.

α_0 – Angle of Bending before Springback ... [°]	ρ – Density ..... [g/cm³]
α_1 – Angle of Bending after Springback ..... [°]	σ_e – Engineering Yield Stress ..... [MPa]
ε – Relative Strain ..... [%]	φ_x – True Strain in the length direction …….. [-]
μ – Coefficient of friction ..... [-]	φ_y – True Strain in the width direction ……..... [-]
v – Poisson coefficient ..... [-]	φ_z – True Strain in the Sheet thickness direction . [-]

Source: Elaborated by authors (2026).

6. Conclusion

For the air bending process of steels of standard EN 10149-2 S700MC and S900MC it is concluded that:

According to the results calculated for True Strain (φ_x) in the outer bending region in the length direction (x), by the analytic method, using Equations 8 and 9, the main methods currently available in the literature to calculate this parameter for the air bending process, it is found to consider only the variables Sheet thickness (s), Punch Radius (r_p) and Bending radius of the midline (r_m), does not take into account mechanical properties of the materials. Furthermore, according to the values calculated regarding the experimental results being between -3.7% to -27.0% for the S700MC steel and -11.8% to -34.5% for the S900MC steel. Using these equations may cause possible errors in predicting this parameter for these two steels, thus indicating for this process and for high-strength steels, the need to formulate an equation to calculate True Strain (φ_x) in the outer bending region in the length direction (x).

In order to predict the Springback Factor (K) using the analytic method of calculation for these two steels, it is appropriate to utilize Equation 11, since the results found regarding experimental analysis were very close, below 10%.

The predictability of the Bending Force (F_d) with the analytical method of calculations, utilizing Equation 13 for those two steels is not indicated, since the results calculated remained below those obtained in the experimental analysis, ranging from -10.0% to -34.1% for the S700MC steel and -28.8% to 38.3% for the S900MC steel.

REMUNOM
ISSN 2178-6925

Received: 13.01.2026 - **Accepted:** 05/06/2026
Vol: 01.03
DOI: 10.61164/7da3gw86
Pages: 1-23

For these two steels, based on the results found, and not considering those of the S900MC steel bended with the Punch Radius (r_p) 3mm, since fissures occurred in the outer bending region, it is suggested to utilize computer simulation using the SIMUFACT FORMING 15® software to predict True Strain (φ_x), as well as for the Springback Factor (*K*) and for Bending Force (F_d), since the percentages of differences in relation to experimental analysis are below 10%.

References

AERENS, R.; MASSELIS, S. Air bending. Scientific and Technical Research Center of the Metal Fabrication Industry (CRIF/WTCM/SIRRIS) MC 110, Leuven, Belgium, 2000.

ALTAN, Taylan & TEKKAYA, A. Erman. *Sheet Metal Forming: Fundamentals*. Materials Park: ASM International, 2012.

AROLA, A-M.; KESTI, V.; RUOPPA, R. The effect of punch radius on the deformation of ultra-high strength steel in bending. Key Eng Mater 639: p. 139-146. 2015.

ASSOCIAÇÃO BRASILEIRA DE NORMAS TÉCNICAS. **ABNT NBR ISO 7438**: Materiais metálicos - Ensaio de dobramento. Rio de Janeiro: ABNT, 2022.

DIETER, G. E. Mechanical Metallurgy. 2nd. ed. New York, McGraw-Hill, p 1-609. 1981.

EUROPEAN STANDARD**. EN 10149-2/2013**: Hot Rolled Flat Products Made of High Yield Strength Steels for Cold Forming – Part 2: Technical Delivery Conditional for Tehrmomechanically Rolled Steels, p. 1-29: EN, 2013.

FARSI, M. A.; AREZOO, B. Bending Force and Spring-Back in V-Die-Bending of Perforated Sheet-Metal Components. Technical Papers • J. Braz. Soc. Mech. Sci. & Eng. 2011.

FU, Z.; MO, J.; CHEN, L.; CHEN, W. Using genetic algorithm-back propagation neural network prediction and finite-element model simulation to optimize the process of multiple-step incremental air-bending forming of sheet metal. Mater Des 31 (1):267-277, 2010.

HOSFORD, W.; CADDELL, R. Metal Forming Mechanics and Metallurgy. 4ª Ed.,

REMUNOM
ISSN 2178-6925

Received: 13.01.2026 - **Accepted:** 05/06/2026
Vol: 01.03
DOI: 10.61164/7da3gw86
Pages: 1-23

New York: Cambridge University Press, p. 30-37. 2011.

LANGE, K. Handbook of metal forming. McGraw-Hill Book Company, New York, US, p. 723-755. 1985.

LEDENTSOY, D.; DÜSTER, A.; VOLK, W.; WAGNER, M.; HEINLE, I.; RANK, E. Model adaptivity for industrial application of sheet metal forming simulation. Finite Elem Anal Des 46 (7):585-600, 2010.

LIVATYALI, H.; ALTAN, T. “Prediction and elimination of Springback in straight flanging using computer aided design methods: Part 1”. Experimental Investigations. J. of Mat. Proc. Tech., Vol. 117(1-2), p. 262–268. 2001.

NARAYANASAMY, R.; PADMANABHAN, P. Comparison of regression and artificial neural network model for the prediction of springback during air bending process of interstitial free steel sheet. J Intell Manuf 23 (3), p. 357-364. 2012.

PERKA, A. *et al*. Advanced High-Strength Steels for Automotive Applicantions: Arc and Laser Welding Process, Properites, and Chalenges, Metals. V. 12, 2022.

ROCHA, R. P.; RIFFEL, M.; MOZETIC, H.; SCHAEFFER, L. Análise do Retorno Elástico no Processo de Dobramento em “V” em Aços de Alta Resistência. Brazilian Journal of Development. v.8, n.4, p. 27662-27677. Abril, 2022.

RODRIGUES, J.; MARTINS, P. Tecnologia Mecânica: Tecnologia da deformação plástica - aplicações industriais. Lisboa: Escolar, p. 265-332, 2010.

SCHAEFFER, L.; NUNES, R. M.; BRITO, A. M. Tecnologia da estampagem de chapas metálicas. 1ª ed. Porto Alegre: Gráfica da UFRGS, p. 56-65. 2017.

SSAB - Swedish Steel AB [homepage on the Internet] 2021. [cited 2023 Dez 18]. Available from: https://www.ssab.com/Products/Brands/Strenx/Products/.

ULSAB. UltraLight Steel Auto Body – Advanced Vehicle Concepts (ULSAB-AVC). [homepage on the Internet] 2017. [cited 2023 Dez 18]: <http://www.worldautosteel.org/projects/ulsab-avc-2/>.

USIMINAS. Usinas Siderurgicas de Minas Gerais. [homepage on the Internet] 2021. [cited 2023 Dez 20]. Available from: https://www.usiminas.com/catalogos/.

VORKOV, V. *et al*. Experimental Investigation of Large Radius Air Bending. The

REMUNOM
ISSN 2178-6925

Received: 13.01.2026 - **Accepted:** 05/06/2026
Vol: 01.03
DOI: 10.61164/7da3gw86
Pages: 1-23

International Journal of Advanced Manufacturing Technology, V. 92. p. 3553-3569. 2017.

VORKOV, V. *et al*. Analytical Prediction of Large Radius Bending by Circular Approximation. Journal of Manufacturing Science and Engineering. V. 140, nº. 12. p. 121010-0 a 121010-12. 2018.

YANG, X. *et a*l. Investigating springback in bending of advanced high-strength steel, Part II Springback prediction. STAMPING J January/February:8-9, 2011.